General Disclaimer

One or more of the Following Statements may affect this Document

- This document has been reproduced from the best copy furnished by the organizational source. It is being released in the interest of making available as much information as possible.

- This document may contain data, which exceeds the sheet parameters. It was furnished in this condition by the organizational source and is the best copy available.

- This document may contain tone-on-tone or color graphs, charts and/or pictures, which have been reproduced in black and white.

- This document is paginated as submitted by the original source.

- Portions of this document are not fully legible due to the historical nature of some of the material. However, it is the best reproduction available from the original submission.

NASA TECHNICAL MEMORANDUM

NASA TM-75228

LOW-CYCLE FATIGUE TESTING METHODS

H. P. Lieurade

Translation of: "Les Méthodes d'Essai en Fatigue Oligocyclique", Mecanique Materiaux Electricite, No. 323-324, November, 1976, pp. 15-26

NATIONAL AERONAUTICS AND SPACE ADMINISTRATION
WASHINGTON, D. C. 20546 MARCH 1978

STANDARD TITLE PAGE

1. Report No. NASA TM-75228	2. Government Accession No.	3. Recipient's Catalog No.
4. Title and Subtitle: LOW-CYCLE FATIGUE TESTING METHODS		5. Report Date: March 1978
		6. Performing Organization Code
7. Author(s): H. P. Lieurade		8. Performing Organization Report No.
		10. Work Unit No.
9. Performing Organization Name and Address: SCITRAN, Box 5456, Santa Barbara, CA 93108		11. Contract or Grant No. NASw-2791
		13. Type of Report and Period Covered: Translation
12. Sponsoring Agency Name and Address: National Aeronautics and Space Administration, Washington, D.C. 20546		14. Sponsoring Agency Code

15. Supplementary Notes

Translation of: "Les Méthodes d'Essai en Fatigue Oligocyclique", Mecanique Materiaux Electricite, No. 223-324, November, 1976, pp. 15-26

16. Abstract

The good design of highly stressed mechanical components requires the accurate knowledge of the service behaviour of materials.

This report gives the main methods for solving the problems of designers:

- determination of the mechanical properties of the material after cyclic stabilization;
- plotting of resistance to plastic deformation curves;
- effect of temperature on the life on low cycle fatigue;
- simulation of notched parts behaviour.

17. Key Words (Selected by Author(s))	18. Distribution Statement
	Unclassified - Unlimited

19. Security Classif. (of this report)	20. Security Classif. (of this page)	21. No. of Pages	22. Price
Unclassified	Unclassified	34	

LOW-CYCLE FATIGUE TESTING METHODS

by H. P. Lieurade
IRSID

Proper sizing of highly-stressed mechanical components requires precise knowledge of in-service behavior of materials: /15*

This report presents the primary methods that make it possible to solve the problems of manufacturers:

- determination of the stable mechanical characteristics of the material;
- plotting resistance to cyclic plastic deformation;
- effect of temperature on low-cyle fatigue life;
- simulation of the behavior of notched specimens.

Author's English Abstract

Low-Cycle Fatigue Testing
The good design of highly-stressed mechanical components requires the accurate knowledge of the service behavior of materials.
This report gives the main methods permitting to solve the problems of designers:
-determination of the mechanical properties of the material after cyclic stabilization;
- plotting of resistance to plastic deformation curves;
- effect of temperature on the life on low-cycle fatigue;
- simulation of notched parts behavior.

Translator's Note: The author often uses the word "deformation" instead of "strain" in much of this article.

*Numbers in margin indicate pagination in original foreign text.

INTRODUCTION

Increasingly high in-service loads and decreasing safety coefficients imposed during the design of mechanical parts submitted to cyclic stresses require accurate knowledge of the behavior of materials used in mechanical constructions.

Some areas of a highly-stressed mechanical part can then be the seat of plastic deformations, particularly in the case of an important change in cross-section (fillets, shoulders) or at right angles to assembly points of the part (holes, weld).

Two questions are therefore asked of the metallurgist and of the mechanic as well during the selection of the closely similar steels to be used:

- What are the stable metallic properties of the material after applying high-stress cycles?
- What is the lifetime of a part or structure submitted to such stresses?

In fact, we know that mechanical properties (elastic limit, work-hardening coefficient) of a material such as steel are greatly modified by applying high-stress cycles, even in a small number. Steel can then either harden or soften as compared with its behavior under constant stress.

It is therefore important to determine the new stress-strain relationships which account for changes in the behavior of materials as soon as they are subjected to cyclic stresses.

Using these relationships, it then becomes possible to define with certainty the maximum acceptable level of design stress for proper operating conditions of a mechanical assembly.

Moreover, low-cycle fatigue tests provide knowledge on the lifetime of parts and structures subjected to high stresses, as well as determining laws giving the number of cycles before rupture, for given cyclic plastic deformation rates.

1 - TESTING METHODS

Compared with standard endurance tests where it it is generally sufficient to measure and control the applied load, plastic fatigue tests require the introduction of a new parameter: metal deformation.

For all types of low-cycle fatigue testing, it is always necessary to measure the deformation of the specimen and often to impose it on the specimen. This is why this type of testing requires significant and often costly equipment.

1.1 Testing Machines

Low-cycle fatigue tests are performed in tension-compression either for a required force, or a required deformation, or still by requiring a given function of strain and stress to retain a fixed value for each stress cycle.

To be able to perform such tests, it is necessary to have a machine with a control loop. Servo-controlled electro-hydraulic machines are particularly well suited for this type of test. /16

With these machines, stress is applied to the specimen with a hydraulic jack controlled with a servo valve. This servo valve receives a signal from the function generator modulated by the control box and corrected at every instant of time by the error function between the control signal and the response signal from the measurement sensor.

Low-cycle fatigue tests are most often performed at low frequencies (< 0.1 Hz) to avoid all parasitic heating of the specimen and, with a triangular-shaped cycle, to have a constant load and deformation speed.

1.2 Test Specimens

1.2.1 Types of specimen

The majority of low-cycle fatigue tests require the application of a stress in the plastic region under compression. That is why we most often resort to very compact specimens with a sufficiently low (≤ 2)"useful length-to-diameter (or width)" ratio to avoid buckling.

- Specimen with a Threaded Grips

It is the most common specimen type: the useful part is either cylindrical (Figure 1a), or with a toric shape (Figure 1b). In the first case specimen deformation is measured along the stress axis; in the second, we transversally measure diameter variations against applied stresses. To avoid thread rupture we generally select a threated section 3 to 5 times longer than the useful section. On the other hand, fillets must be sufficiently large to avoid rupture at the junction area.

- Flat specimens (Figure 2)

To avoid specimen buckling when going into compression, it is mandatory to reinforce the specimen here and there. To allow the specimen to stretch freely, an anti-friction plate is placed between the specimen and the anti-buckling device.

1.2.2 Anchoring specimens

The anchoring of specimens requires certain precautions so as to eliminate deflection components that can increase possibilities of buckling the specimen.

That is why it is recommended that, before each test, the axiality of anchor heads whose alignment errors must be reduced (< 0.05mm) must be checked.

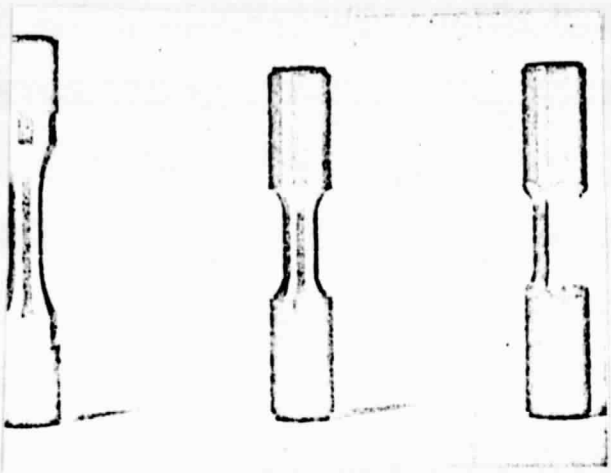

a) Longitudinal Reference Measurement

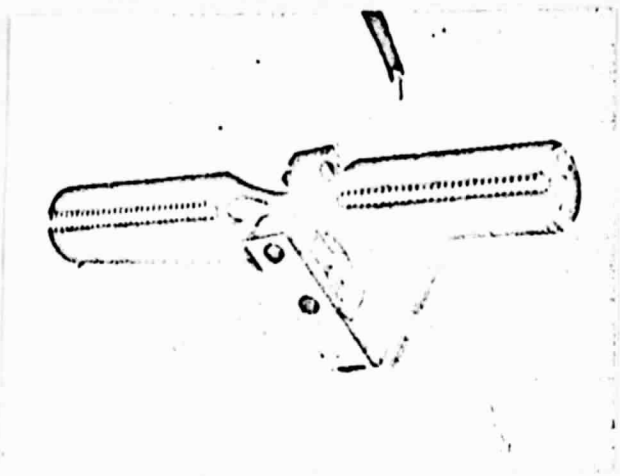

b) Diameter Reference Measurement

Figure 1: Fatigue Test Specimens with threaded heads.

To make possible an optimum alignment, some experimenters use metal anchors as described by Wood (1). With the specimen installed on the machine, the specimen is introduced into the bridle bits in a liquid state and provides specimen anchoring without parasitic stresses after solidifying.

1.3 Devices for Measuring Forces and Deformations

1.3.1 Force Sensor

Forces are most often measured with a load cell placed at the end of the specimen anchor. These cells are composed of either a deformation sensor gauge or a sensor using inductance variations.

1.3.2 Deformation Sensor

There are two types of extensiometers (2) to measure the deformation of the specimen: some are directly attached to the specimens while the others make no contact.

- Extensiometers attached to the specimen (Figure 3):

Different commercially-available types use either deformation gauges or inductance coils. These sensors deliver an electric voltage that varies linearly with the separation of the knife blades applied to the specimen and, therefore, with the elongation of the latter. Their main characteristics are a negligible amount of drifting over a period of time, satisfactory static calibration, a negligible hysteresis error and a correct frequency response up to 20 Hz. To avoid slippage of the sensor blades, either during loading, or during the first cycles, we can either glue onto the specimen some adhesive tape pierced through by the sensor blades, or apply varnish to the points of contact between the blades and the specimen after installing the sensor on the specimen.

- Contactless Extensiometers: /17

They are generally optical extensiometers using either an ordinary light or a laser beam.

1.3.3 Case of Toric specimens

In the case where we impose a diametral deformation amplitude, $\Delta\varepsilon_d$, test results are often analyzed in terms of total longitudinal deformation $\Delta\varepsilon_t$ in the following manner:

$$\Delta\epsilon_t = \frac{\Delta\sigma}{E}\left(1 - \frac{\nu_e}{\nu_p}\right) + \frac{\Delta\epsilon_d}{\nu_p}$$

where ν_e and ν_p are Poisson's elastic and plastic coefficients, respectively, for the material

$\Delta\sigma$ is the stress amplitude

E is Young's Modulus

1.4 Devices for Hot Tests

To simulate the low-cycle fatigue behavior of materials working while heated in the plastic region, it is indispensable to perform tests at operating temperatures. The specimen is heated, either with an electric oven or by induction using a small coil fed driven by a high-frequency generator and cooled with water (Figure 4).

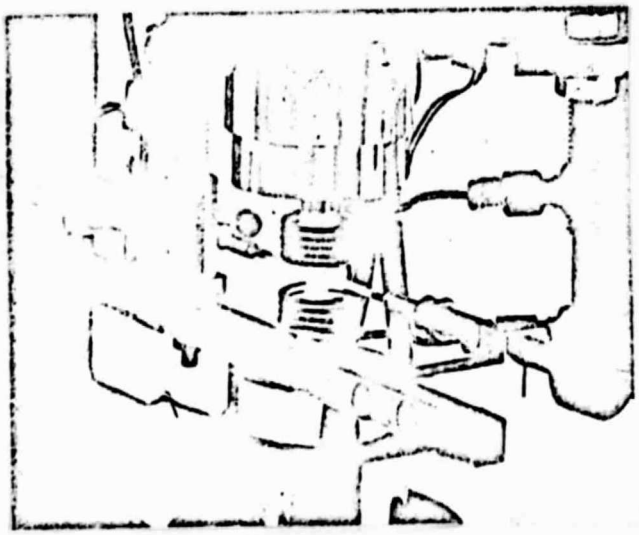

Figure 4. Hot Test Device

In the first case, the knife blades placed against the specimen are integrated with non-expanding reference rods that make it possible to measure specimen deformation from outside the oven.

In the case of induction heating, two alumina knife blades provide the measurement of diameter changes of the specimen.

Figure 2. Anti-Buckling Device in the Case of a Flat Specimen

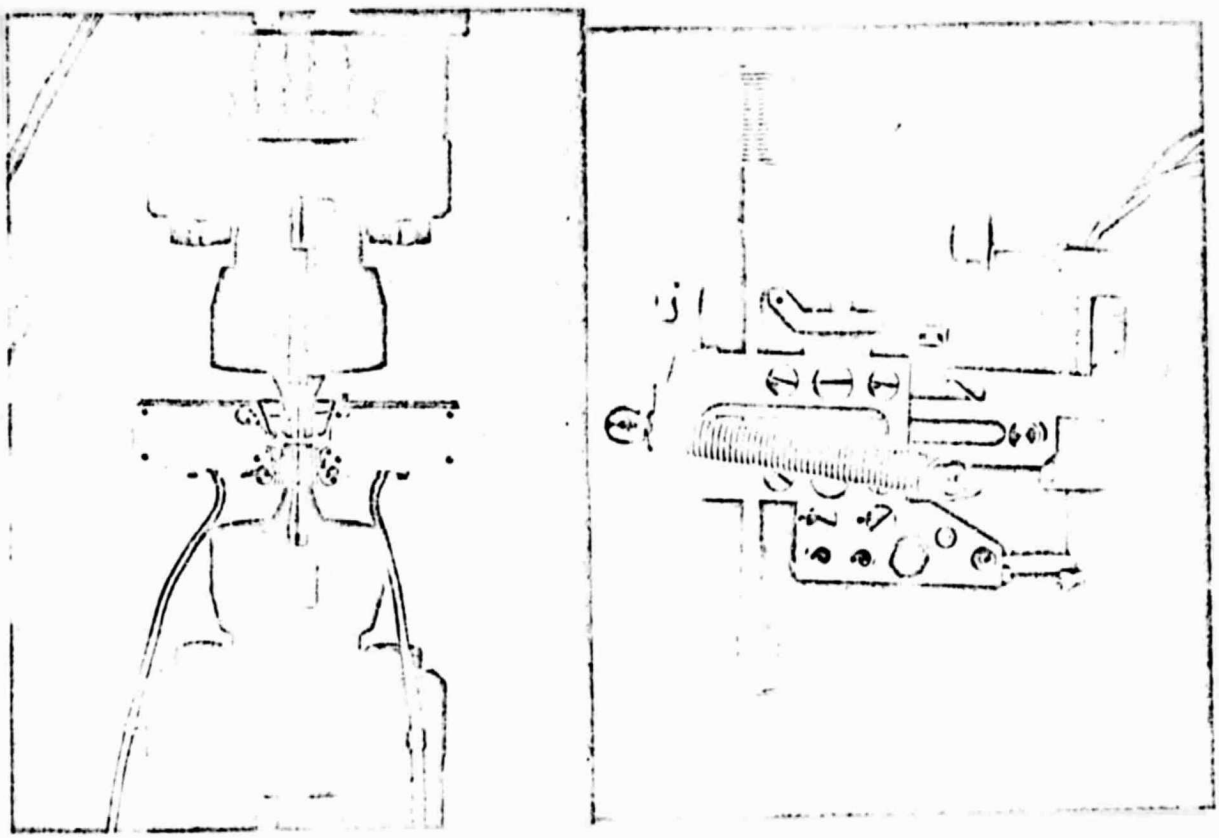

a) Double sensor, with Deformation Gauge

b) Induction Coil sensor

Figure 3. Elongation Sensor Used in Axial Loaded Fatigue

2 - CYCLIC COLD-WORK CURVES

The study of the evolution of the stress-strain relationship during stress cycles, particularly near the elastic limit is often the object of much interest on the part of designers. Indeed, the plot of the cyclic curve makes it possible to determine some stable characteristics of the material such as the elastic limit R'_e and the cold-work coefficient n'.

Several methods are proposed (3) to determine the "cyclic traction curve" obtained after the stabilization of mechanical characteristics. These appreciably different methods have the purpose of adapting the metal under study to alternating (traction-compression) total deformation cycles of variable levels applied by the test machine. /18

a) Method by Increments

In this method which requires the use of a curve follower, we apply to the material a series of amplitude steps for increasing and then decreasing deformation. Figure 5 shows the variation in strain obtained.

The cyclic traction curve is then the locus of the maximum points on the mechanical hysteresis loops (Figure 5b) corresponding to the stability of the material. Generally, this stability is obtained after 3 or 4 steps of about 60 cycles. In the case of the steel illustrated, we observe (Figure 5c) a softening of the steel.

b) Method using a specimen per level

In this case, we plot the cyclic traction curve one point at a time. Each point represents the maximum of the hysteresis layer obtained from a specimen after the constraint has stabilized.

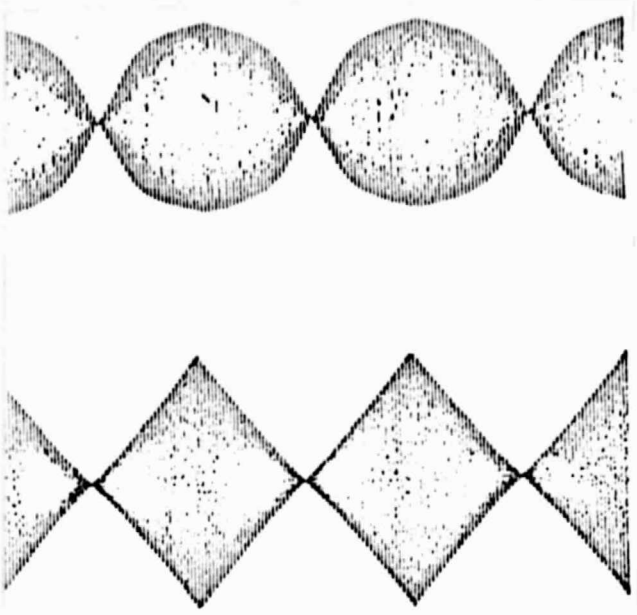

a) Variation of the applied strain (lower) and of stress (upper) as a function of time

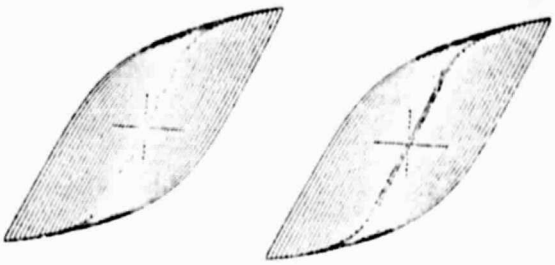

b) Evolution of Hysteresis Loops (ordinate), e= Δ l (abscissa)

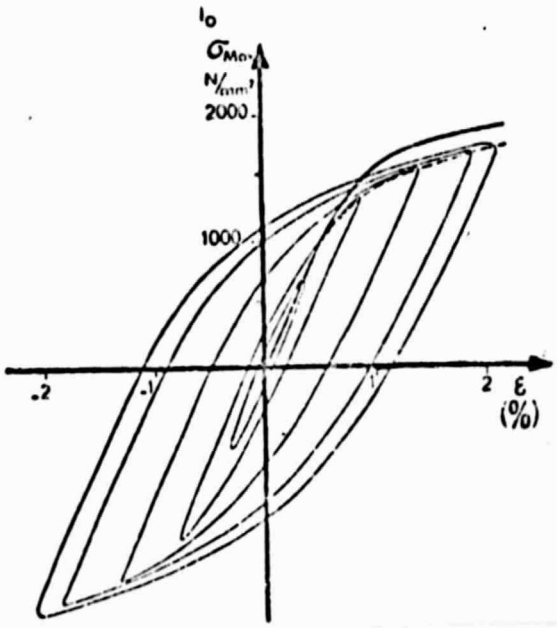

c) Plot of the Cyclic Curve shown with a dotted line. Plot of the Constant Traction shown as a solid line

Figure 5. Determination of the Cyclic Traction Curve. Deformation Increment Method.

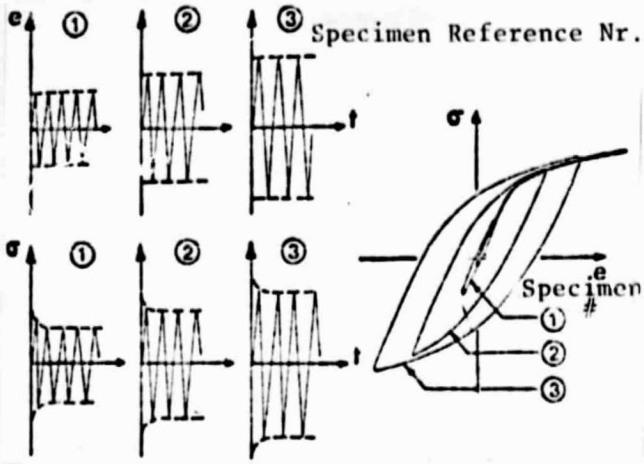

Figure 6. Determination of the Cyclic Traction Curve: Test Method a specimen per applied level of deformation.

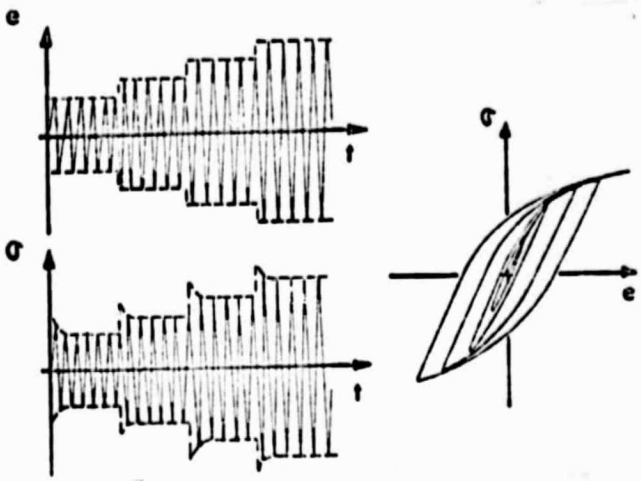

Figure 7. Determination of the Cyclic Traction Curve: Test Method Using Different Consecutive Levels (staircase) with the Same Specimen.

c) Method Using Different Consecutive Levels (Staircase)

Here, we only use a single specimen which is stressed at different but increasing levels of deformation (Figure 7). At each level, we wait for the strain to stabilize before recording the cycle as stable and before going to the next level. /19

d) Traction After Cycling

After using the increment method and, therefore, after adapting the metal to a variable deformation amplitude, we can, after the stress has stabilized and after returning to zero strain and stress, perform a traction test (Figure 8 on the next page).

e) Half Hysteresis Loop

We can also apply directly a high amplitude stress directly (Figure 9). The stable hysteresis loop is then transferred to a system of axes with the origin at the maximum point of the loop and all scale values divided by two.

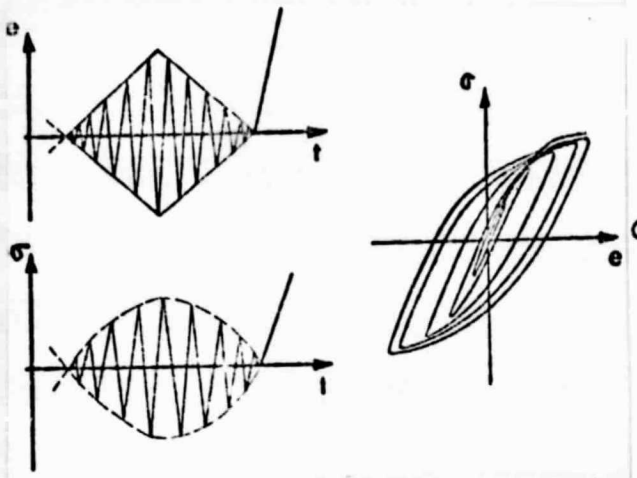

Figure 8. Determination of the Cyclic Traction Curve Through a Traction Test After Cycling

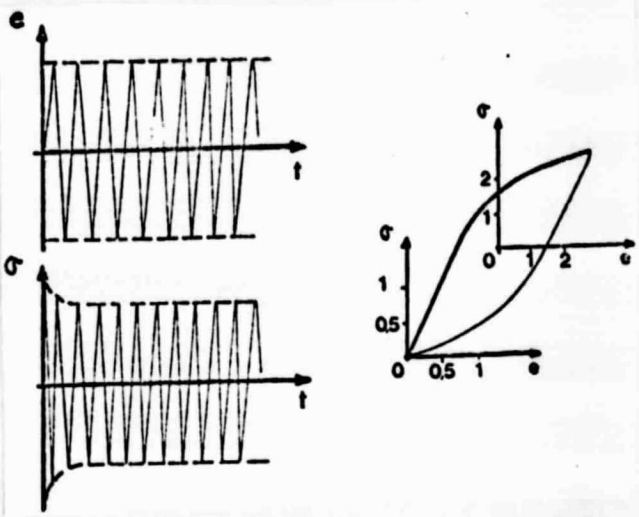

Figure 9. Determination of the Cyclic Traction Curve Using the Hysteresis Loop Section Corresponding to the Rising Portion of the Cycle

2.2 Comparison of Determination Methods

Recent studies performed at IRSID over a wide range of steels (4)(5) have shown the effect of the method on the plot of cyclic cold-work curves performed up to a total deformation of ±2%.

- In the case of high-resistance steels ($R_m \sim 2{,}000$ N/mm^2), tempered and annealed, which soften during testing, the first three methods give similar results (Figure 10)

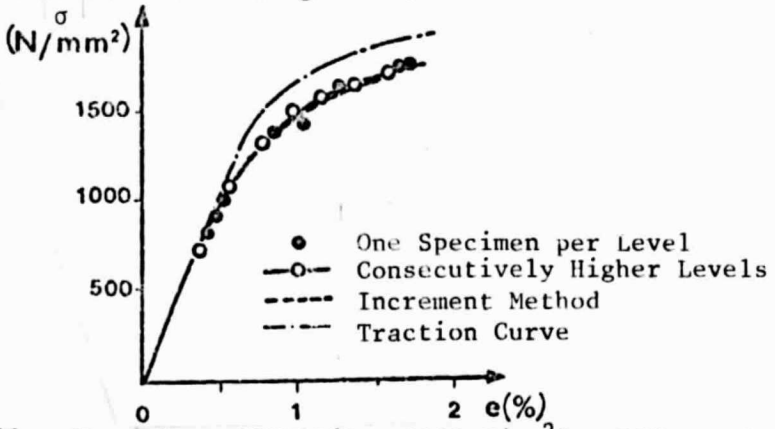

Figure 11. Steel Type 35CD16($R_m \sim 2000$ N/mm^2). Effect of the cyclic Curve Determination Method.

In the case of medium-resistance steels ($R_m \sim 1{,}000$ N/mm^2), we can note that, for small plastic deformations, the curves obtained by using a specimen per level and the one obtained by consecutive levels with the same specimen are appreciably higher than those obtained with the increment method (Figure 11).

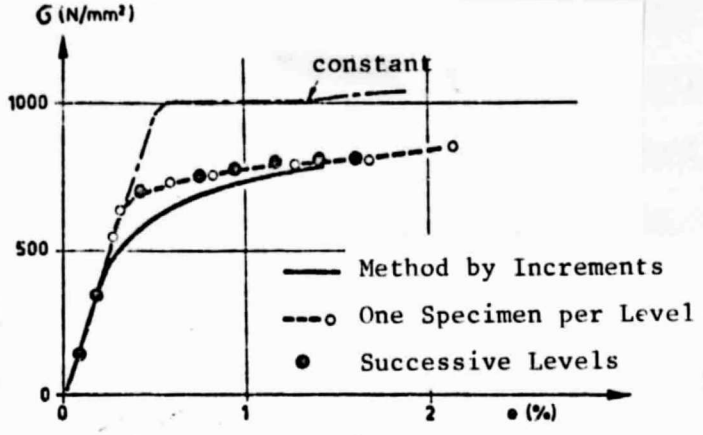

Figure 11. Steel Type 35CD4 (R_m 1,000). Effect of the Cyclic Curve Determination Method.

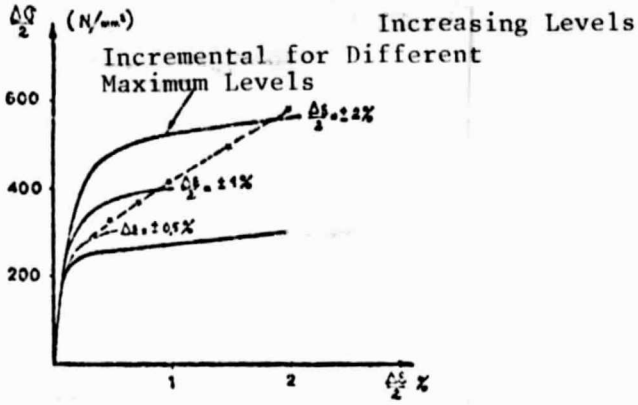

Figure 12. Comparison of the Cyclic Curve for Consecutive Levels (Dashed Line) and for the Incremental Method for Different Levels of $\Delta\varepsilon_t$ (Steel Type Z6CND 17-12)

- In the case of a stainless steel of Type Z6CND 17-12 (AISI 316), we observe a significant hardening (Figure 12 on the previous page). The curves obtained by increment are a function of the maximum deformation reached. Curves obtained with methods b) and c) then pass through the maximum points of cyclic cold-work curves determined by the increment method. /20

2.3 PROCESSING RESULTS

To determine parameters k' and n' of the cyclic cold-work law: $\sigma_r = k' \epsilon_r^{n'}$

we transfer onto a log-log diagram the rationalized strain:

$$\sigma_r = \frac{F}{S_o}(1 + e_p)$$

where F is the recorded force

S_o is the initial cross-section of the specimen

e_p is the measured plastic elongation

as a function of the true deformation: $\varepsilon_r = \log e\ (1 + e_p)$

K' and n' are respectively the ordinate at the origin and the slope of the straight line through the points.

2.4 EFFECT OF TEST PARAMETERS (ambient temperature)

2.4.1 - Frequency and shape of the load cycle.

In the case of tests performed in ambient temperature, we do not observe a significant effect of frequency, or the deformation speed or the cycle shape on the plot of the cyclic cold-work curve (6).

The effect of stress velocity can, however, be important in the case of tests performed at a high temperature. In this case, creep or relaxation phenomena add themselves to plastic fatigue mechanisms (7).

2.4.2 - Deformation Ratio $R_\varepsilon = \frac{\varepsilon_{min}}{\varepsilon_{max}}$

In a conventional manner, the determination of the cyclic force-deformation curve is performed for a total deformation ratio

$$R_\varepsilon = \frac{\varepsilon_{min}}{\varepsilon_{max}} = -1$$

To study the effect of R_ε we can stress a specimen with a ratio $R_\varepsilon = 0$, that is to say with a zero minimum elongation of the specimen.

The sketch of Figure 13 shows the evolution of the hysteresis loop during the first cycles: this evolution takes into consideration, on the one hand, the softening of the metal which tends to acquire stable mechanical characteristics and, on the other hand, the relaxation of the average strain which tends to approach a zero value (8).

On the diagram of Figure 13*, we have plotted the points $(\frac{\Delta\sigma}{2}, \frac{\Delta\varepsilon_t}{2})$ corresponding to the stabilization of the tested steel 35CD4 specimens (annealed at 600°C) and the curve established with the same method (one specimen per level) for $R_\varepsilon = 1$. The points fall onto the curve and show a negligible effect of R_ε on the plot of the cyclic traction curve.

---

* Translator's note: The author actually referred to Figure 14.

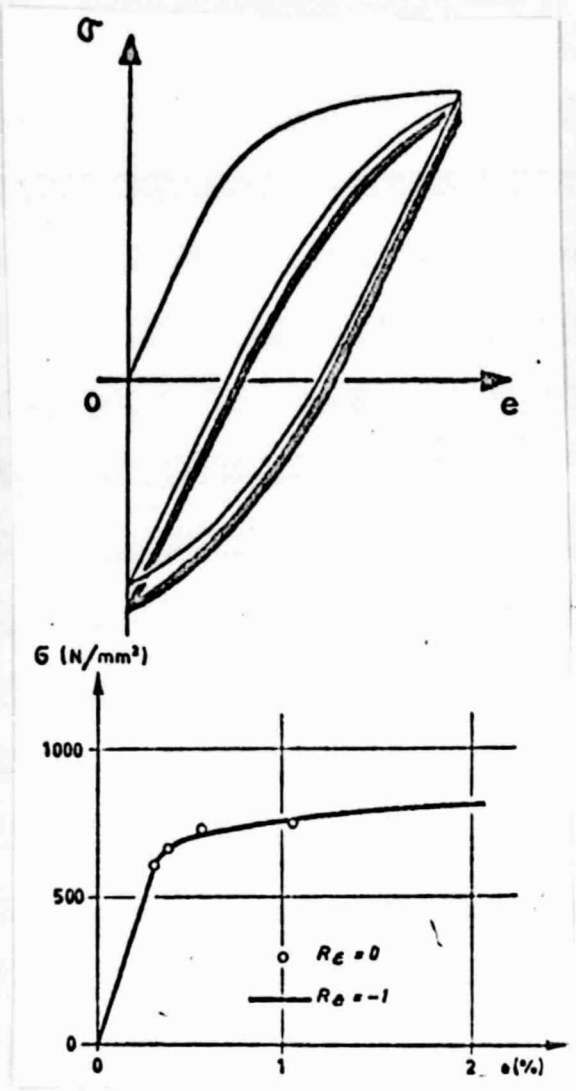

Figure 13. Effect of the Deformation Ratio on the Plot of the Cyclic Curve. 35CD4 Steel (annealed at 600°C).

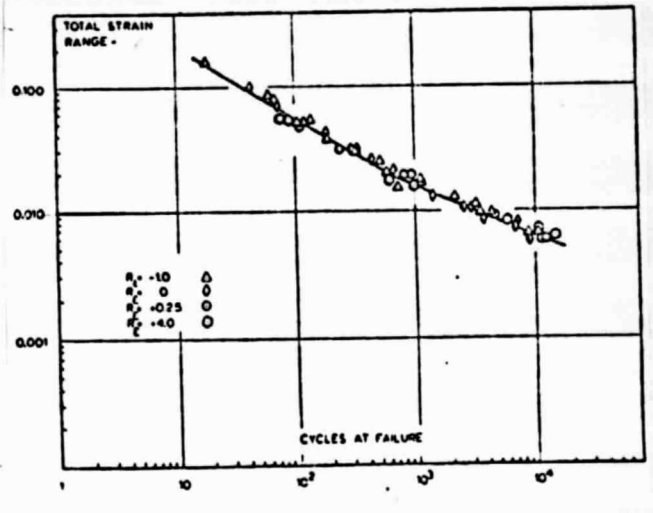

Figure 14. Effect of R_ε on the Curve $\varepsilon = f(N)$ for a Steel with 9% Ni.

3 - LOW-CYCLE FATIGUE RESISTANCE CURVES

/21

These curves plotted from fatigue-to-failure tests are called "Manson-Coffin" curves. They make it possible to determine the laws relating elastic, plastic and total applied stresses to the life of the specimens.

3.1 Measured Parameters

Figure 15 shows the evolution of strain with an increasing number of cycles for different constant levels of total stress for the case of a "maraging" steel annealed at 500°C for 4 hours. This evolution reflects three stages: a significant decrease of strain during the first ten cycles, then a more or less slow decrease over more than 90% of the life, and finally, a rapid drop in strain leading to failure.

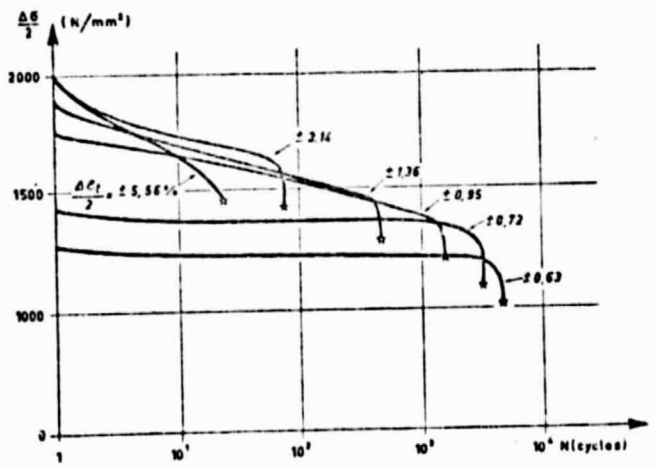

Figure 15: Evolution of Strain Amplitude as a Function of the Number of Cycles for Different Levels of Applied $\Delta\varepsilon_t$.
Maraging Steel (Annealed at 500°C for 4 hours)

Although, usually, the amplitude of total deformation $\Delta\varepsilon_t$ remains constant during the test, since it is applied, the amplitude of plastic deformation $\Delta\varepsilon_p$ changes as cycles increase in number, as does the amplitude of elastic deformation $\Delta\varepsilon_e$.

To show the effect of plastic and elastic deformation amplitudes on the life of specimens, we are led to define a reference mechanical hysteresis loop on which we measure these parameters.

- For low deformations leading to lifetimes greater than 200 cycles, we generally select the hysteresis loop for the 50th cycle.

- In the case of high deformations, we agree to take the cycle that corresponds to the half-way point of drop or increase in strain amplitude.

We then report the values for $\frac{\Delta\varepsilon_t}{2}$ $\frac{\Delta\varepsilon_p}{2}$ and $\frac{\Delta\varepsilon_e}{2}$ on a log-log diagram: $\frac{\Delta\varepsilon}{2} = f(N)$ (Figure 16).

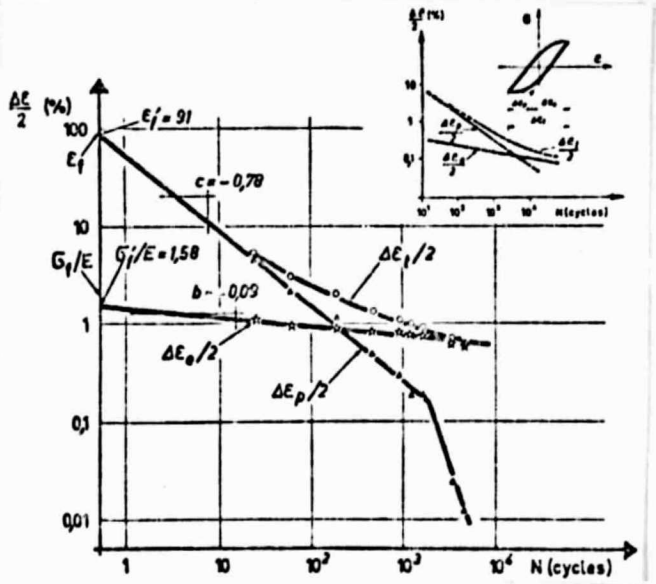

Figure 16: Lifetime as a Function of Elastic, Plastic and Total Deformations. Maraging Steel (Annealed at 500° for 4 Hours).

3.2 Determination of Low-Cycle Fatigue Resistance Laws

3.2.1. Lifetime as a Function of Stress

On the $\frac{\Delta\varepsilon}{2}$ – N (Number of cycles to fatigue) diagram in Figure 16 we have recorded, for each specimen made of maraging steel annealed at 500°C, the $\frac{\Delta\varepsilon_t}{2}$ $\frac{\Delta\varepsilon_p}{2}$ and $\frac{\Delta\varepsilon_e}{2}$ levels measured on the reference hysteresis loop as a function of lifetime:

- the points corresponding to elastic deformation are located on a straight line with slope b (index of resistance to fatigue). Elastic deformation for ½ cycle corresponds to σ'_f/E where E is Young's Modulus and σ'_f is the resistance coefficient to fatigue;
- points corresponding to plastic deformation are located on a straight line with slope c (index of fatigue ductility). The deformation level ε'_f for ½ cycle (coefficient of fatigue ductility) is the true deformation that causes the failure in one half-cycle;
- points corresponding to total deformation are located on a curve asymptotic to "elastic" and "plastic" straight lines.

3.2.2. Expression of Low-Cycle Fatigue Resistance Laws

- Properties of Fatigue Resistance

The "elastic" straight line makes it possible to determine coefficients b and σ'_f in the relationship:

$$\frac{\Delta\varepsilon_e}{2} = \frac{\sigma'_f}{2}(2N)^b$$

which can also be written, according to Basquin's Law (9), as: /22

$$\frac{\Delta\sigma}{2} = \sigma'_f (2N)^b$$

- Properties of Fatigue Ductility

The "plastic" straight line makes it possible to know coefficients c and ε'_f in Manson's relationship (10):

$$\frac{\Delta\varepsilon_p}{2} = \varepsilon'_f (2N)^c$$

- Relationship between Total Deformation and Lifetime

The curve representing total deformation as a function of lifetime follows the equation:

$$\frac{\Delta\epsilon_t}{2} = \frac{\Delta\epsilon_e}{2} + \frac{\Delta\epsilon_p}{2} = \frac{\sigma'_f}{2}(2N)^b + \epsilon'_f(2N)^c$$

3.3 EFFECT OF TESTING CONDITIONS

3.3.1. Frequency and Shape of the Stress Cycle

Various authors (5)(11) (12) have studied the effect of deformation speed and the shape of the stress cycle and they have shown that, at an ambient temperature, these parameters had no significant effect on specimen life provided the test frequency was sufficiently low to avoid a noticeable heating of the specimen.

3.3.2. Deformation Ratio R

In the case of steel specimens with 9% Ni, Dubuc and colleagues (13) varied R_ε between -1 and +4 and found no noticeable effect of this parameter (Figure 14). These results have been confirmed with very high-resistance and medium-resistance steels, by Gallet and Lieurade (4)(5).

Indeed, as we have shown in paragraph 2.4.2., the evolution of the hysteresis loop is very rapid during the first cycles; this evolution takes into account not only the softening of the metal which seeks to find stable mechanical characteristics but more importantly, a relaxation of average stress which quickly tends to a zero value. This is why the cyclic traction curve obtained after a few hundred cycles is the same regardless of R_ε. In the same manner, during a test to failure, the rapid evolution of the hysteresis loop during the first cycles is sufficiently rapid so that there is no effect of R_ε on specimen life.

3.4 DISSIPATED ENERGY

Many researchers (14 through 17) have attempted to use mechanical hysteresis

energy as a criteria for fatigue damage.

Indeed, we know that, at the microscopic level, cyclic plastic deformation is associated with the movement of dislocations and that cyclic strain relates to their displacement.

That is why cyclic plastic deformation and cyclic strain are both necessary for damage to take place by causing dissipation of mechanical energy.

Thus plastic deformation energy per cycle can be considered as a measure of fatigue damage per cycle and fatigue resistance of a metal can be described in terms of the capacity to absorb and dissipate plastic deformation energy.

It is possible to relate both plastic deformation energy per cycle and total energy of deformation-to-failure to life.

For each test, we can measure the energy per cycle by measuring the area of the hysteresis loop corresponding to the reference cycle. This energy per cycle, ΔW, as well as the total deformation energy to failure $W_f = \Delta W \cdot N$ (N: number of cycles to failure at the level studied), both expressed in Joules/mm^3, are recorded on log-log diagrams in Figure 17, in the case of different types of high-resistance steels (5).

In the first case, we note a significant decrease of energy per cycle, ΔW, when the number of cycles increases.

On the other hand, we observe a slight increase of total energy to failure W_f when N increases.

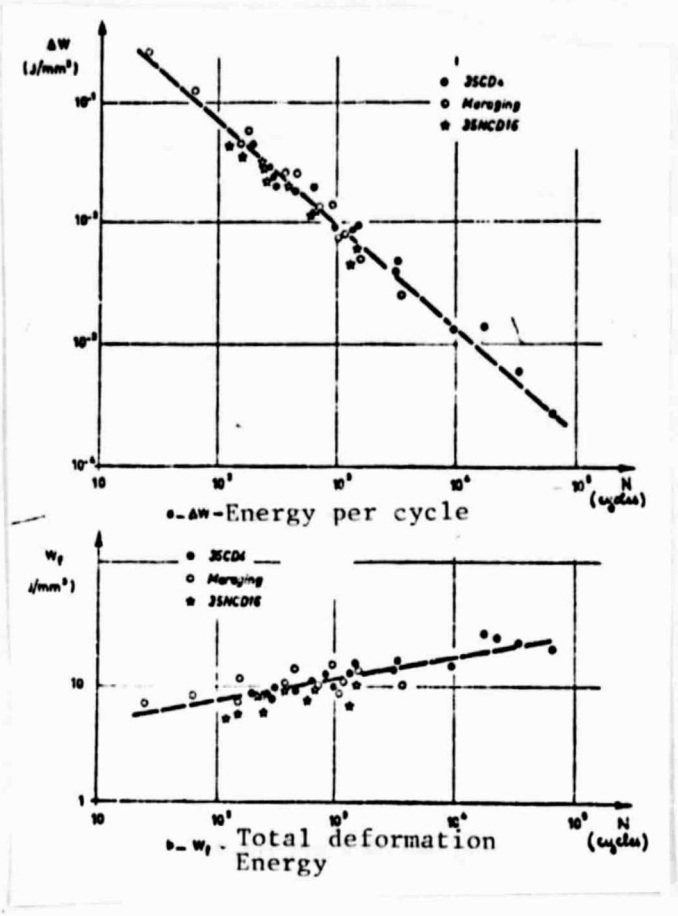

Figure 17. Evolution of plastic deformation energy as a function of lifetime.

In this case, points align themselves on straight lines described by equations: /23

$$\Delta W = A \cdot N^{a-1} \text{ and } W_f = A \cdot N^a$$

where A = 3.2 J/mm^3 and a = 0.15.

Instead of measuring the area of the mechanical hysteresis loop for the reference cycle, we can also use the relationship proposed by Halford (18):

$$\Delta W = \Delta\sigma \cdot \Delta\epsilon_p \left(\frac{1-n'}{1+n'}\right)$$

Knowing n', on the one hand, and the reference cycle plastic deformation and strain amplitude on the other, it is possible to know with good accuracy the amount of plastic deformation energy dissipated per cycle, using the preceding relationship.

4 - CASE OF HIGH-TEMPERATURE TESTS

Over the last several years, many projects bear on the behavior of materials and particularly on stainless steels subjected to cyclic plastic deformations applied at high temperatures.

4.1. Cyclic Cold-Work Curves

The first area of application of this research is devoted to the study of the evolution of the stress-strain deformation, in particular in the neighborhood of its elastic limit.

Jaske and his collaborators (19) have determined the cyclic curves for a stainless steel of type 304, between 20 and 700°C. Thus, they have brought to light the effect of test conditions and particularly of the deformation speed and the maximum deformation level during metal adaptation. In the same manner, Berling and Slot (20) have shown that, at a high temperature, the cyclic characteristics of AISI 304 steel and particularly $R'_{e_{0,2}}$ decrease when the deformation speed decreases by a factor of 10 to 100 and that the temperature increases from 430 to 816°C.

To bring out the effect of test frequency ν at a given temperature, Coffin (21)(22) has proposed the following relationship between the stress

amplitude and the amplitude of plastic deformation $\Delta\varepsilon_p$, corresponding to the stabilized cycle:

$$\Delta\sigma = A\,\Delta\varepsilon_p^{\,n'} \cdot \nu^{k_1}$$

The advantage of this relationship is shown on the diagram of Figure 18 where we have plotted the $\Delta\sigma \cdot \nu^{-K_1}$ points which correspond to frequencies betwen 4×10^{-3} and 4×10^{-5}/sec for each value of $\Delta\varepsilon_p$. At each test temperature points align themselves on the same straight line regardless of the test frequency.

4.2 Low-Cycle Fatigue Resistance Curves

In the case of tests to failure, various studies have shown that the deformation speed (frequency)(20) and hold times had a significant effect on low-cycle fatigue of stainless steels at high temperature(21).

The introduction of hold time at the maximum deformation level of the fatigue cycle as well as the decrease of deformation speed reduce fatigue life: the rate of decrease is then related to the combined effect of the hold time and of the decrease in deformation speed. Essentially, all studies published on this subject confirm these effects whose importance depends on various factors such as the type of metal, temperature, deformation amplitude and the shape of the deformation cycle. In this case, lifetime depends on the position of hold time during the cycle (traction or compression).

Generally, results are expressed using a relationship derived from Manson-Coffin's law (24 to 26):

$$\Delta\epsilon_p = C\,(N\nu^{k-1})^{-\beta}$$

where t'_c = time for $\frac{1}{2}$ cycle

t'_h = hold time for each cycle.

$$\nu = \frac{1}{t'_c + t_h}$$

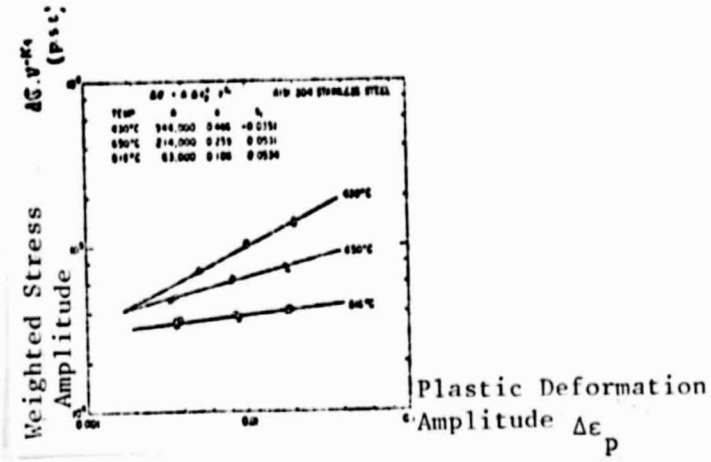

Interaction of frequency and stress level on the plastic deformation level at different temperatures and different frequencies.

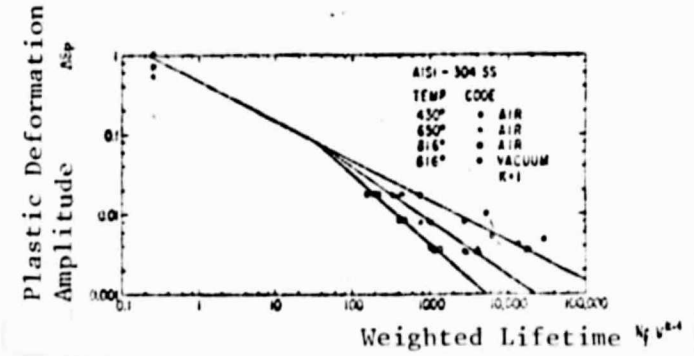

Presentation of test results on a diagram of deformation amplitude against lifetime modified by frequency.

Figure 18: Low-Cycle Fatigue Test Results at High Temperature.

On the $\Delta\varepsilon_p = f(N\nu^{k-1})$ diagram of Figure 18b we have plotted the test points obtained at different temperatures with a Type 304 steel for three deformation speeds 4×10^{-3}, 4×10^{-4} and 4×10^{-5}/sec. For each temperature, the points align themselves well along straight lines, thus showing the validity of the relationship proposed by Coffin. /24

Similarly, Coffin expresses the elastic deformation amplitude by the relationship:

$$\Delta\epsilon_e = \frac{\Delta\sigma}{E} = \frac{A'}{E} N^{-\beta'} \nu^{k'_1}$$

where $A' = AC^{n'}$ $\beta' = \beta^{n'}$ and $k'_1 = \beta^{n'}(k-1) + k_1$

5 - SIMULATION OF NOTCH BASE (27)

Some stressed structure elements in the elastic region often possess metal discontinuities where the stress level can exist the plastic region. That is why an elastoplastic analysis of the stress and strain field is essential to validly predict the lifetime of components. Numerous analyses have been proposed; Neuber's appears the most interesting one.

In his study, Neuber relates the cyclic load amplitude of a notched part to the stress and true deformation at the bottom of the notch and he then estimates the lifetime of the notched part from the -N or -N curves obtained with smooth specimens. Neuber's rule is the following:

$$K_t^2 = K_\sigma \cdot K_\epsilon$$

where K_t is the stress concentration factor in material behavior elastic model.

K_σ is the stress concentration factor in the elasto-plastic model

K_ϵ is the strain concentration factor in the same model.

This formula has been checked by Morrow and his collaborators (29) by replacing K_t with the fatigue notch factor K_f. The modified Neuber's rule then becomes:

$$K_f^2 = K_\sigma \cdot K\epsilon$$

With the help of this relationship, these authors have checked with an aluminum alloy that it is possible to simulate with good accuracy tests on notched specimens while using smooth specimens by knowing the K_f coefficient. In particular, they have shown that for a notched specimen tested under a nominal stress $\Delta\sigma_{nom}$ less than the elastic limit, the notch bottom is submitted to a stress-strain state such that:

$$\Delta\sigma \cdot \Delta\epsilon \cdot E)^{1/2} = K_f \cdot \Delta\sigma_{nom} = \text{constant}$$

As an example, Figure 19 shows the evolution of cycles during testing according to Topper's model (29). The cycles are arranged between two branches that the author considers as stable during testing.

We observe perfect agreement between the curve $(\Delta\sigma \cdot \Delta\epsilon \cdot E)^{1/2} = f(N)$ obtained with smooth specimens (Figure 20) and the curve $(K_f \cdot \Delta\sigma_{nom}) = f(N)$ determined with notched specimens. According to Topper, et al (30), the proposed method is limited to the initiation of cracks or to final failure in the case where the crack stage is negligible. It is starting with a similar analysis that, recently, Baus and his collaborators (31) have studied the initiation of fatigue cracks on very high-resistance steel specimens with shape defects and different dimensions. The elasto-plastic criteria that they propose, based on low-cycle fatigue results obtained with smooth specimens, confirm results obtained with notched specimens.

CONCLUSION

Low-cycle fatigue results satisfy current needs of designers when they have to design parts or structures totally stressed in the plastic region (tanks under pressure, landing gears) or with mechanical discontinuities (holes, welds), seats of stress concentrations. /25

In these types of test, it is necessary to measure and often to apply the deformation amplitude to the specimen. That is why these tests

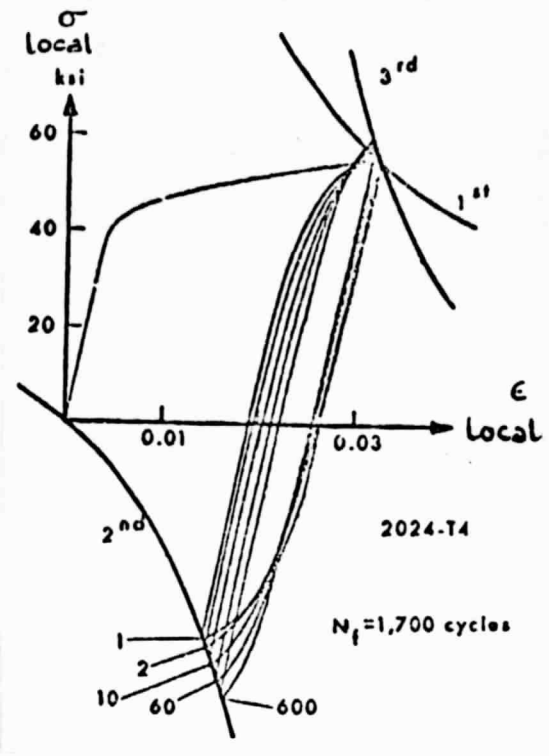

Figure 19: Recording of the simulation of elasto-plastic behavior of a notch by using a smooth specimen.

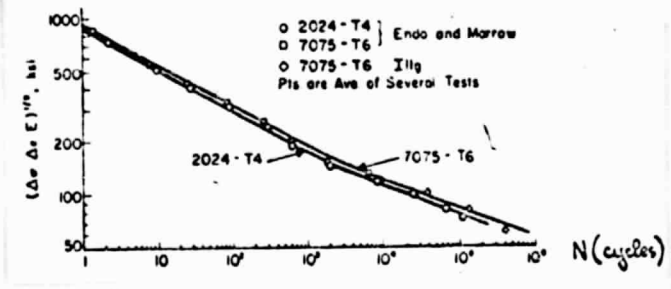

Figure 20a. Results with smooth specimens

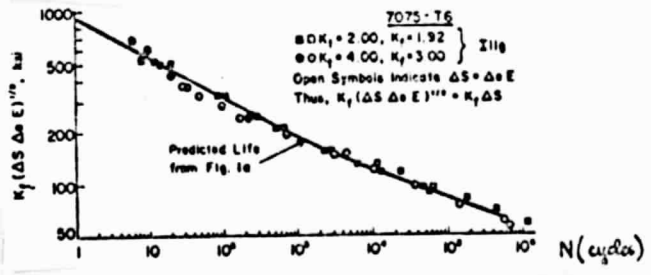

Figure 20b. Comparison of results obtained with notched specimens and of the predicted curve using smooth specimens (Figure 21a)

require test machines and instrumentation that are very advanced and therefore costly.

Different methods make it possible to account for the behavior of highly-stressed materials in service:

- when computing structures, the plot of cyclic cold-work makes it possible to use stable characteristics relative to cyclic deformations;
- the deformation of the parameters in Manson-Coffin's law:

$$\frac{\Delta\epsilon_p}{2} = \epsilon'_f (2N)^b$$

  makes possible the prediction of the number of cycles to failure N as a function of plastic deformation amplitude to which the part or structure is subjected;
- in the case of notched parts, it is possible to predict with accuracy their lifetime, using test results obtained with smooth specimens.

BIBLIOGRAPHY

(1) Feltner (C.E.), Mitchell (M.R. - Basic Research on the Cyclic Deformation and Fracture Behavior of Materials -Publication ASTM STP 465, pp. 27-60 , 1969.

(2) Handbook of Fatigue Testing - Publication ASTM STP 560, 1974.

(3) L.E. Feltner, R.W. Landgraf - Selecting Mateials to Resist Low-Cycle Fatigue - ASME Paper Nr. 69, DE 59, 1969.

(4) G. Gallet, H.P. Lieurade - Influence of the Metalographic Structure of a Nickel-Chromium-Molybdenum Steel on its Plastic Fatigue Behavior- Report IRSID RE 236 - Mem. Scient. Rev. Met., April 1976, pp. 219-240.

(5) G. Gallet, H.P. Lieurade - Low-cycle Fatigue Behavior of Different Steels with Very High and Medium Resistance such as types Maraging and 35 CD4 - Report IRSID RE 000 - C.I.T. from the C.D.S. (to be published).

(6) Benson (D.K.), Hancourk (J.R.) - The Effect of Strain Rate on the Cyclic Response of Metals - Met. Trans., Vol. 5, August 1974, pp. 1711-1715.

(7) Abdel-Raouf (H), Plumtree (A), Topper (T.H.) - Effects of Temperature and Deformation Rate on Cyclic Strength and Fracture of Low-Carbon Steel - Publication ASTM STP 519, 1973, pp. 28-57.

(8) R.W. Landgraf - The Resistance of Metals to Cyclic Deformation - Publication ASTM, STP 467, 1970, pp. 3-36.

(9) O.H. Basquin - The exponential Law of Endurance Tests - Proceedings American Society Testing Mats, Vol. 10, Part II, 1910, pp. 625-630.

(10) S.S. Manson - Machine Design - M.A.D.E.A. 7, 1960, p.139.

(11) Massarelli (L), Ranucci (D.) - Influenza della frequenza e della forma d'onda del carico sulla fatiga oligociclia - Metalurgia Italiana - October 1970

(12) Gucer (D.E.), Sapa (M) - Frequency Effects in Low-Cycle-Fatigue - Metallurgical Transactions, Volume 1, November 1970, pp. 3075-3081.

(13) Dubuc (J), Vanasse (J.R.), Biron (A.), Basergui - Evaluation of Pressure Vessel Design Criteria for Effects of Means Stress in Low-Cycle Fatigue - Proceedings of the First International Conference on Pressure Vessel Technology (Delft- 1969), Part II, pp. 1253-1266.

(14) Inglis (N.P.) - Hysteresis and Fatigue of Wohler Rotating Cantilever Specimen - The Metallurgist, February 1927, pp. 23-27.

(15) Miner (M.A.) - Cumulative Damage in Fatigue - Transactions, Am. Soc. Mechanical Engineers, Volume 67, 1945, p. A 159.

(16) Morrow (J.D.) - Cyclic Plastic Strain Energy and Fatigue of Metals.

(17) Bui-Quoc (T.) - Cyclic Stress, Strain and Energy Variation under Cumulative Damage Tests in Low-Cycle Fatigue - Journal of Testing and Evaluation, Volume 1, January 1973, pp. 58-64.

(18) G.R. Halford - The Energy Required for Fatigue - Journal of Materials Volume 1, Nr. 1, March 1966, pp. 3-18.

(19) C.E. Jaske, H. Mindlin, J.S. Perrin - Cyclic Stress-Strain Behavior of Two Alloys at High Temperature - Publication ASTM STP 519, 1973, pp. 13-27.

(20) J.T. Berling, T. Slot - Effect of Temperature and Strain Rate on Low-Cycle Fatigue Resistance of AISI 304, 316 and 348 Stainless Steels - Publication ASTM STP 549, pp. 3-30.

(21) L.F. Coffin - The Effect of Frequency on the Cyclic Strain and Low-Cycle Fatigue Behavior of Cast Udimet 500 at Elevated Temperature- Metallurgical Transactions, Volume 2, 1971, p. 3105.

(22) L.F. Coffin - Fatigue at High Temperature - Publication ASTM STP 520, 1973, pp. 5-34.

(23) CF Cheng, C.Y. Cheng, D.R. Dierks, R.W. Weeks - Low-Cycle Behavior of Types 304 and 316 Stainless Steel at LMFBR Operating Temperature- Publication ASTM STP 520, 1973, pp. 355-364.

(24) J.B. Conway, J.T. Berling, R.H. Stentz - Strain Rate and Holdtime Saturation in Low-Cycle Fatigue: Design-Parameter Plats - Publication ASTM STP 520, 1973, pp. 637-647.

(25) SS. Manson - Fatigue: A Complex Subject - Sample Simple Approximations /26
Experimental Mechanics, Volume 5, Nr.7, July 1965, pp. 193-226.

(26) S.S. Manson - The Challenge to Unify Treatment of High-Temperature Fatigue. A Partisan Proposal Based on Strain Range Partitioning - Publication ASTM STP 520, 1973, pp.744-782.

(27) L.F. Coffin, R.M. Goldhoff - Predictive Testing in Elevated Temperature Fatigue and Creep: Status and Problems - Publication ASTM STP 515, 1972, pp. 22-74.

(28) Effects of Notches on Low-Cycle Fatigue (A Literature Survey) - Publication ASTM STP 490, May 1972.

(29) Neuber (H), Theory of Stress Concentration for Shear-Strained Prismatic Bodies with Arbitrary Non-Linear Stress-Strained Low - Journal of Applied Mechanics, Vol. 28, Nr. 4, December 1961, pp. 544-550.

(30) Morrow (J.D.), Wetzel (R.M.), Topper (T.H.) - Laboratory Simulation of Structural Fatigue Behavior - Publication ASTM STP 462, 1970, pp. 74-91.

(31) Topper (T.H.), Wetzel (R.M.), Morrow (J.D.) - Neuber's Rule Applied to Fatigue of Notched Specimen - Journal of Materials JMLSA, Vol. 4, Nr. 1, May 1969, pp. 200-209.

(32) Baus (A), Lieurade (H.P.), Sanz (G), Truchon (M.) - Study of Fatigue Crack Initiation on Very High-Resistance Steel Specimens with Shape Defects and Different Dimensions - Report IRSID P 260 - Revue de Métallurgie (Metallurgy Magazine) (To be published).